*NAR Genomics and Bioinformatics*, 2024, **6**, lqae060
https://doi.org/10.1093/nargab/lqae060
Advance access publication date: 30 May 2024
**Standard Article**

# G-quadruplex propensity in *H. neanderthalensis, H. sapiens* and Denisovans mitochondrial genomes

**Václav Brázda [1,2,*], Lucie Šislerová [1,2], Anne Cucchiarini [3] and Jean-Louis Mergny [1,3,*]**

[1]Institute of Biophysics of the Czech Academy of Sciences, Královopolská 135, 612 00 Brno, Czech Republic
[2]Brno University of Technology, Faculty of Chemistry, Purkyňova 118, 612 00 Brno, Czech Republic
[3]Laboratoire d'Optique et Biosciences (LOB), Ecole Polytechnique, CNRS, INSERM, Institut Polytechnique de Paris, 91120 Palaiseau, France

[*]To whom correspondence should be addressed. Tel: +420 541 517 231; Fax: +420 541 211 293; Email: vaclav@ibp.cz
Correspondence may also be addressed to Jean-Louis Mergny. Email: jean-louis.mergny@inserm.fr

## Abstract

Current methods of processing archaeological samples combined with advances in sequencing methods lead to disclosure of a large part of *H. neanderthalensis* and Denisovans genetic information. It is hardly surprising that the genome variability between modern humans, Denisovans and *H. neanderthalensis* is relatively limited. Genomic studies may provide insight on the metabolism of extinct human species or lineages. Detailed analysis of G-quadruplex sequences in *H. neanderthalensis* and Denisovans mitochondrial DNA showed us interesting features. Relatively similar patterns in mitochondrial DNA are found compared to modern humans, with one notable exception for *H. neanderthalensis*. An interesting difference between *H. neanderthalensis* and *H. sapiens* corresponds to a motif found in the D-loop region of mtDNA, which is responsible for mitochondrial DNA replication. This area is directly responsible for the number of mitochondria and consequently for the efficient energy metabolism of cell. *H. neanderthalensis* harbor a long uninterrupted run of guanines in this region, which may cause problems for replication, in contrast with *H. sapiens*, for which this run is generally shorter and interrupted. One may propose that the predominant *H. sapiens* motif provided a selective advantage for modern humans regarding mtDNA replication and function.

## Introduction

*Homo neanderthalensis* and Denisovans are close extinct relatives who became extinct approx. 40,000 years ago. Genetic relationships between Hominins remained a mystery for a long time (1,2), as obtaining accurate genomic information on ancient hominins was complicated by the small number of samples that were free of microorganisms or human DNA contamination and of sufficient quality (3,4).

After *H. neanderthalensis* mitochondrial DNA (mtDNA) was completely sequenced, it became apparent that its mtDNA did not fall within the range of modern human mtDNA variation, suggesting that *H. sapiens* and *H. neanderthalensis* never interbred (5–7). However, after sequencing of *H. neanderthalensis*' nuclear genomes, evidence emerged that interbreeding did occur between *H. sapiens* and *H. neanderthalensis* (3,4,8,9). This exchange of genes may have happened several times, including during the period when humans first started migrating from Africa to Europe and Asia, which were already inhabited by *H. neanderthalensis* and *Denisovans* (10,11). In 2008, Pääbo *et al.* discovered a previously unknown hominin, which was given the name Denisovan, based on a 40,000-year-old fragment from a finger bone discovered in the southern part of Siberia (12). Its exceptionally well-preserved DNA allowed to obtain a high-coverage genome which appeared unique when compared to *H. neanderthalensis* and present-day humans (8).

Today's non-African humans carry approximately 2% (with values reported between 1 and 4%) of *H. neanderthalensis* genome sequences in their nuclear genome (4,5,12–14). The relationship between *Denisovans* and *H. sapiens* has first been reported in populations in Melanesia and other parts of South East Asia, where individuals carry up to 6% *Denisovans* DNA. The genetic makeup of modern humans may have benefited from encountering *H. neanderthalensis* and *Denisovans* (3,9). Studies suggest that this admixture in the genome of modern humans had an impact on our immune response to different types of infections, helping us adapt to the pathogens present in newly settled areas. Moreover, *H. neanderthalensis* are believed to have possessed genetic elements that encode proteins that interact with RNA viruses (15,16). The Denisovan EPAS1 gene confers an advantage for survival at high altitude and is common among present-day Tibetans (17).

The sequencing of the human genome is an important and fascinating scientific journey that began in the 1990s, but was first published in 2001, which involved scientists from all over the world who collaborated to identify and map out more than 3 billion base pairs that form the human genome (18,19) 'completed' over two decades ago. However, until recently, when the gapless telomere-to-telomere (T2T) assembly of human genome was published in 2022 (20), complete information about all chromosomes was missing. Several high-coverage nuclear *H. neanderthalensis* and Denisovans genomes are now available, and at least 25 and 10 complete mitochondrial *H. neanderthalensis* and Denisovans genomes, respectively, have been completely sequenced. This allowed detailed analyses of the variations between

**Received:** December 15, 2023. **Revised:** April 18, 2024. **Editorial Decision:** May 13, 2024. **Accepted:** May 17, 2024

*H. neanderthalensis*, Denisovans and *H. sapiens* genomes, for example to study the evolution of human immunity (21).

G-quadruplexes are secondary DNA structures formed from G-quartets, planar structures formed from four guanines using Hoogsteen bonds, and stabilized by cations such as $K^+$, $Na^+$ or $NH_4^+$ (22–24). The G-quadruplex structure can adopt different molecularities and topologies, including parallel, antiparallel, and hybrid forms, depending on the orientation and arrangement of the strands (one example provided in Figure 1A; more topologies are shown in Supplementary Figure S1). Genomic regions containing stretches of guanine-rich sequences, called G-rich motifs, are prone to form G-quadruplex structures. G-quadruplexes are found in various genomes, including those of humans, other mammals, plants, archaea and bacteria (25–33). G4 have been shown to play an important role in key biological processes such as replication, transcription, translation, mRNA processing, and genome stability (34). For higher eukaryotes, G-quadruplex-forming sequences are abundant in genomic regions, especially telomeres, oncogene promoters, untranslated regions (UTRs) of mRNA, but also in mitochondrial DNA (35–37). Due to their presence in the DNA of proto-oncogenes, they are frequently associated with cancer and may represent suitable therapeutic targets (38–40).

As PQS have been found in almost all organisms and genomes, it is not surprising that they were also present in mtDNA. An exhaustive *in vitro* analysis of over 200 potential G4 sequences in *H. sapiens* mitochondrial DNA has been performed (41). However, limited information is available regarding the functions of these G-quadruplexes in mitochondrial DNA. Direct evidence for the transient presence of G-quadruplexes in mtDNA was recently obtained by Doimo *et al.*, using an engineered G4-binding protein targeted to the mitochondrial matrix of a human cell (42). A comprehensive analyses of mtDNA of various organisms showed that PQS are over-represented in the 3′UTR, D-loops, replication origins and stem loops of mtDNA and G4 sequence in the D-loop is conserved across taxonomic sub-groups (43).

The displacement loop, or D-loop, is a three-stranded region in the non-coding region of mtDNA approximately 650 nt long. This third strand is commonly called 7S DNA. This region in mtDNA is important control region. The origin of replication of the heavy strand is located between nucleotide positions 16,024–16,576, and the origin of transcription for both light and heavy strands is located in the same region. It therfore controls transcription and replication (44). Changes in this control region have also been shown to have a significant effect on mtDNA expression (45,46). A link was also found between D-loops mutation and diseases such as Parkinson's disease, lupus erythematosus, myopathy, Sjögren syndrome, dermatomyositis, rheumatoid arthritis and many others (47–53). Furthermore, mutations in the D-loop are associated with the overall aging of the organism (54). Interestingly, there was also a significant decrease in D-loop methylation, up to complete demethylation in colorectal cancer cells (53).

In this work, we analyzed the presence of G-quadruplexes in the *H. neanderthalensis*, Denisovans and *H. sapiens* (both current and ancient) mitochondrial genomes. We found a similar number of PQS in the mtDNA of these species, with one crucial difference in the D-loop region, which represents an important regulatory site, and for which sequence variations have been found to lead to significant physiological changes in *H. sapiens*.

## Materials and methods

### Sequences

Complete mtDNA genomes can be found in the NCBI database. For statistical purposes, we downloaded all mitochondrial genomes of *H. neanderthalensis*, Denisovans and *H. sapiens* ancient genomes (30,000 years or older) (list of NCBI IDs provided in Supplementary Table S1). For contemporary modern humans, all available mtDNAs (61,261 entries) available on 28 June 2023 at NCBI were used. The reference genome for *H. sapiens* is NCBI ID: NC_012920.1.

### G4Hunter analyses

Data were analyzed using the G4Hunter algorithm, with a window size of 25 nucleotides and a G4Hunter threshold scores of 1.2, 1.6 or 2.0: the higher the threshold, the more likely is the formation of a very stable G4—a score above 1.6 indicates near-certain G4 formation, and 2.0 near certain formation of a heat stable quadruplex (55). The output from the algorithm was exported to a .csv file and the following analyses were performed with the Microsoft Excel software.

### Construction of LOGO sequences

The mt sequences from the *H. neanderthalensis*, Denisovans and *H. sapiens* genomes were uploaded to UGENE software (56). The locations of the PQS were extracted using ClustalW alignment. Using the aligned sequences, the LOGO sequence was generated by employing WebLogo 3 tool (57). For example, a comparison of contemporary and ancient modern humans is provided in Supplementary Figure S2.

### Oligonucleotides and chemicals

DNA Oligonucleotides were ordered from Eurogentec, Belgium and used without further purification. Concentrations were determined using the extinction coefficients provided by the manufacturer. Stock solutions were prepared at 100 μM strand concentration in pure water. All oligonucleotides were annealed in corresponding buffers, kept at 95°C for 5 min and slowly cooled to room temperature before measurements. All chemical reagents were purchased from Sigma-Aldrich (France).

### Analysis of quadruplex formation *in vitro*

To confirm G4 formation, we used a combination of biochemical and biophysical techniques (58). Specifically, G4 thermal stability was analyzed by recording CD spectra at various temperatures, using a JASCO J-1500 (France) spectropolarimeter (scan range: 340–200 nm; scan rate: 100 nm/min; averaging three accumulations). TDS and IDS were recorded by measuring the arithmetic difference between spectra in denaturing conditions (95°C or in absence of potassium respectively) and in G4 promoting conditions (25°C or in presence of potassium). FRET-MC experiments were performed according to (55), by taking the difference of melting temperature between F21T and the tested sequence, with or without PhenDC3, using a Biorad qPCR CFX96 (USA). Fluorescence based methods were performed with two G4 ligands (Thioflavin T (ThT) and N-methyl mesoporphyrin IX (NMM)) as previously described (59), using a TECAN M1000 Pro (Switzerland) plate reader and a Biorad ChemiDoc to read the fluorescence intensity, in a 96-well microplate and in a native

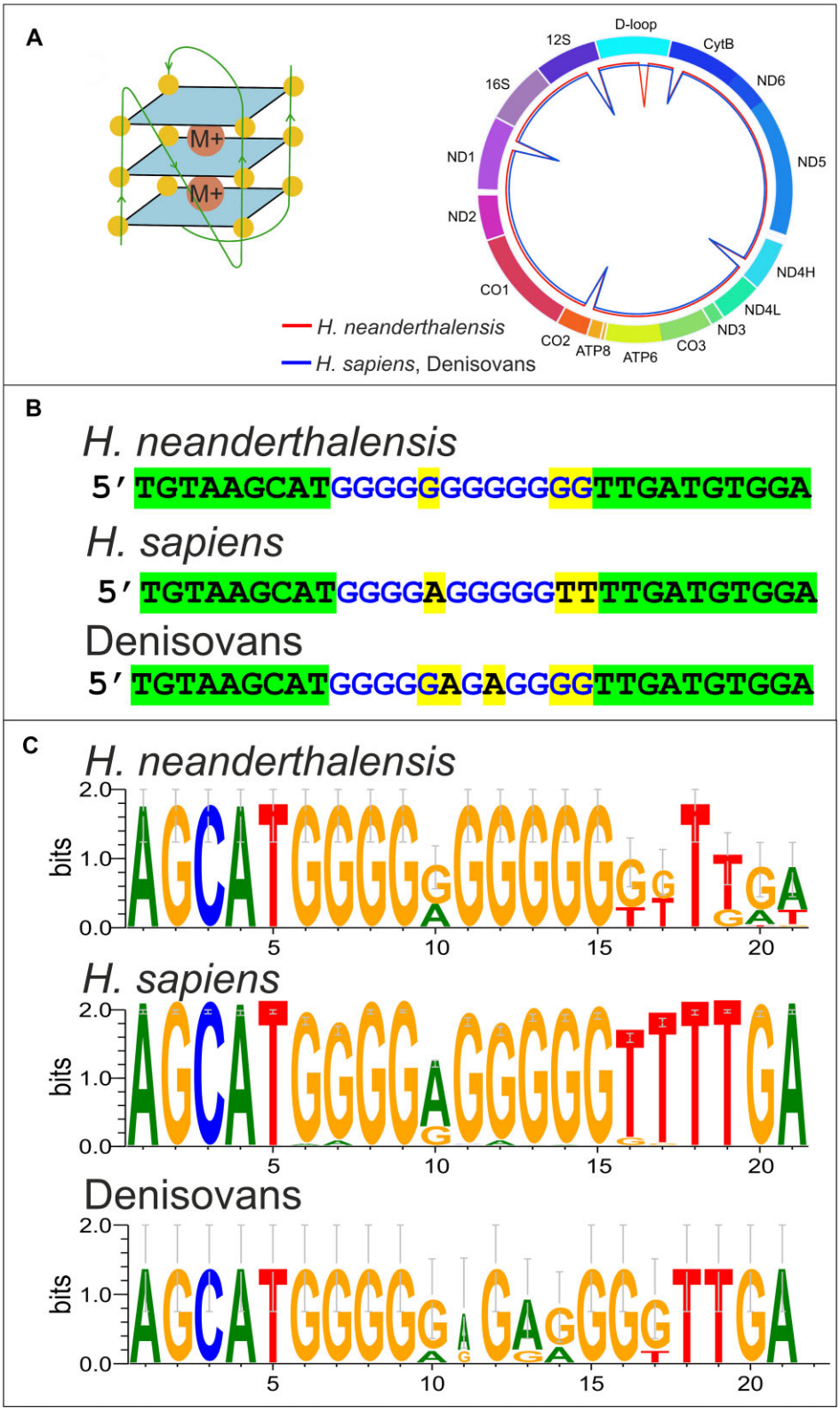


**Figure 1.** Most stable G4-prone sequences in mtDNA. (**A**) *Left:* Example of an intramolecular G-quadruplex topology and *Right*: Position of high stability (G4Hunter score above 2) quadruplexes in mtDNA from *H. neanderthalensis*, Denisovans and *H. sapiens*. The outer circle shows the mtDNA regions, the inner circle show the location of the G4-prone sequences (blue: *H. sapiens* and Denisovans, red: *H. neanderthalensis*). All G4 in *H. neanderthalensis*, Denisovans and *H. sapiens* are in the same location (±5 nt), except for the extra G4 located in the D-loop region only found in *H. neanderthalensis* mtDNA. (**B**) PQS region in D-loop of *H. neanderthalensis*, Denisovans and *H. sapiens* genomes. Sequences from the reference genome for *H. sapiens* (the complementary strand is shown). G-rich regions are shown in blue; surrounding conserved sequences are highlighted in green, while differences within the G-rich region are highlighted in yellow. The G-run is *always* interupted in Denisovans, by one or two adenines. (**C**) Logo sequence from all accessible *H. neanderthalensis*, *H. sapiens* and Denisovans genomes.

**Table 1.** PQS in mtDNA of *H. sapiens* and *H. neanderthalensis*

| Name/G4Hunter threshold | 1.2 | 1.6 | 2.0 |
|---|---|---|---|
| *H. sapiens* | 109 | 30 | 5 |
| *H. neanderthalenis* | 108 | 29 | 6 |
| *Denisovans* | 103 to 106 | 30 or 31 | 5 or 6 |

**Table 2.** mtDNA Sequences tested

| Name | Sequence (5′ ⇒ 3′) | G4H |
|---|---|---|
| 22nG | **AGCATGGGGGGGGGGGTTGAT** | 2.23 |
| 22dG | **AGCATGGGGGAGAGGGGTTGAT** | 1.73 |
| 22sG | **AGCATGGGGAGGGGGTTTTGAT** | 1.68 |
| RSRS | **AGCATGGGGGGAGGGTTTTGAT** | 1.55 |
| 22c | **AGCATGTCGAGAACGTTTTGAT** | 0.14 |

Abbreviations: G4H = G4Hunter score. Higher values correspond to more stable G4s. Sequences with a G4H below 0.8 are extremely unlikely to form a G4. 22nG = *H. neanderthalensis* motif. 22dG: Denisovan motif. 22sG = Homo sapiens motif. 22RSRS = *Reconstructed Sapiens Reference Sequence*. 22c = negative control in which the G-track has been extensively mutated (very low G4H score).

polyacrylamide gel. A DNA ladder (Gene Ruler Ultra Low Range, Thermofisher, USA) was added to the wells.

### Statistical analyses

Results are expressed as mean ± SD. Statistical significance was determined using GraphPad Prism 10 and an unpaired Student's *t*-test. *P*-values are stated in the figure captions. Significance: $*P < 0.05$, $**P < 0.01$; $***P < 0.001$, $****P < 0.0001$.

## Results

### PQS in mitochondrial genomes comparison

First, we compared the occurrence of sequences for G-quadruplex formation in mtDNA. The size of the *H. sapiens* mtDNA reference genome (16,569 bp) is very close to the size of *H. neanderthalensis* and Denisovans mtDNA (16,565 and 16,565 bp, respectively). The difference in the nucleotide sequence is minimal with an identity of 98.72% between *H. sapiens* and *H. neanderthalensis*, according to the BLAST algorithm (60). Similarly, the analysis of PQS occurrence showed that the amount of PQS in *H. sapiens* and *H. neanderthalensis* does not differ significantly (109 and 108 occurrences with a G4Hunter threshold of 1.2, i.e. a modest 0.9% difference). Similar result was obtained with analyses with G4Hunter score above 1.6. However, if we compared the absolute numbers of very stable PQS with a G4Hunter score >2, there are only five occurrences in *H. sapiens* as compared to 6 in *H. neanderthalensis* (Table 1). The situation is a bit more complex in Denisovans: depending on the genome considered, there are five or six motifs.

There is therefore one more high stability PQS in *H. neanderthalensis* than in *H. sapiens*. Unsurprisingly, the five others high stability PQS are located in the same regions of the *H. sapiens*, Denisovans and *H. neanderthalensis* mtDNA genomes. The sixth *H. neanderthalensis* PQS with a G4Hunter score >2 is located in the D-loop of mtDNA (Figure 1A), which is critical for mtDNA replication (44).

### Analysis of the D-loop region

A detailed comparison of the PQS part of the D-loop in *H. neanderthalensiss*, Denisovans and *H. sapiens* genomes shows that the nucleotides surrounding the PQS region are nearly identical (100% identity—shown in green in Figure 1B). The predominant allele in *H. sapiens* (either contemporary or ancient—there are minimal differences between the two, as shown in Supplementary Figure S2) is formed by two separated tracks of five and four consecutive guanines interrupted by an A. The same region in the *H. neanderthalensis* genome is formed by 12 guanines in a row, which is very rare in *H. sapiens* (Figure 1C) and absent in the ten currently available Denisovans genomes (The high G4H score of some Denisovans sequences comes from the presence of a nearby G-track; the sequence context is fundamentally different from *H. neanderthalensis*).

### Quadruplex formation in the D-loop

We anticipated that the changes in sequence between *H. sapiens* and *H. neanderthalensis* in the D-loop region would impact G4 formation. For example, it has been previously shown that sequences containing runs of 12–19 consecutive guanines are capable to form very stable intra and intermolecular G4 structures (61). To verify this prediction, we ordered several families of synthetic 22- (Table 2) or 31- nucleotide-long (Supplementary Figure S7) DNA oligonucleotides mimicking the most frequent alleles of the G-rich sequences around the D-loop. To investigate if these synthetic sequences would form a G-quadruplex or not, we used a combination of biochemical and biophysical techniques, as each individual method has shortcomings (58).

G4H corresponds to the *G4Hunter score* (a higher score means a higher propensity to form a stable G4) *n, d* and *s* stand for *H. neanderthalensis*, Denisovans and *H. sapiens*, respectively. RSRS corresponds to the *Reconstructed Sapiens Reference Sequence* (62). 22c is a control DNA oligonucleotide in which the G-runs have been extensively mutated to prevent G4 formation: its G4Hunter score is very low, very close to 0.

The G-rich strands were tested using a number of independent methods to test G4 formation; the main results are presented in Figure 2, while additional experiments and sequences are displayed in supplementary information. We advocate the use of several independent methods to investigate G-quadruplex formation, as each technique has its own limitation, such as requiring ionic conditions differing from the physiological ones: for example, a lower $K^+$ concentration is needed for FRET-MC. Our results confirmed a higher tendency of the *H. neanderthalensis* sequence to form G-quadruplexes:

- In the FRET-MC assay (Figure 2A), we test the ability of each oligonucleotide to act as a competitor for the binding of a well-known and extensively characterized G4 ligand called PhenDC3 (63). Positive (G4-forming, bcl2, ckit2, cmyc) and negative (single- or double strands, RND6, ds26) controls were included. 22c, the negative control, behaved as expected (no competition). 22nG behaved like the most active positive controls (the smaller the bar, the more efficient is the competition), in agreement with stable G4 formation. In contrast 22sG gave a less efficient competition efficiency, suggesting a lower ability to form a stable G4.

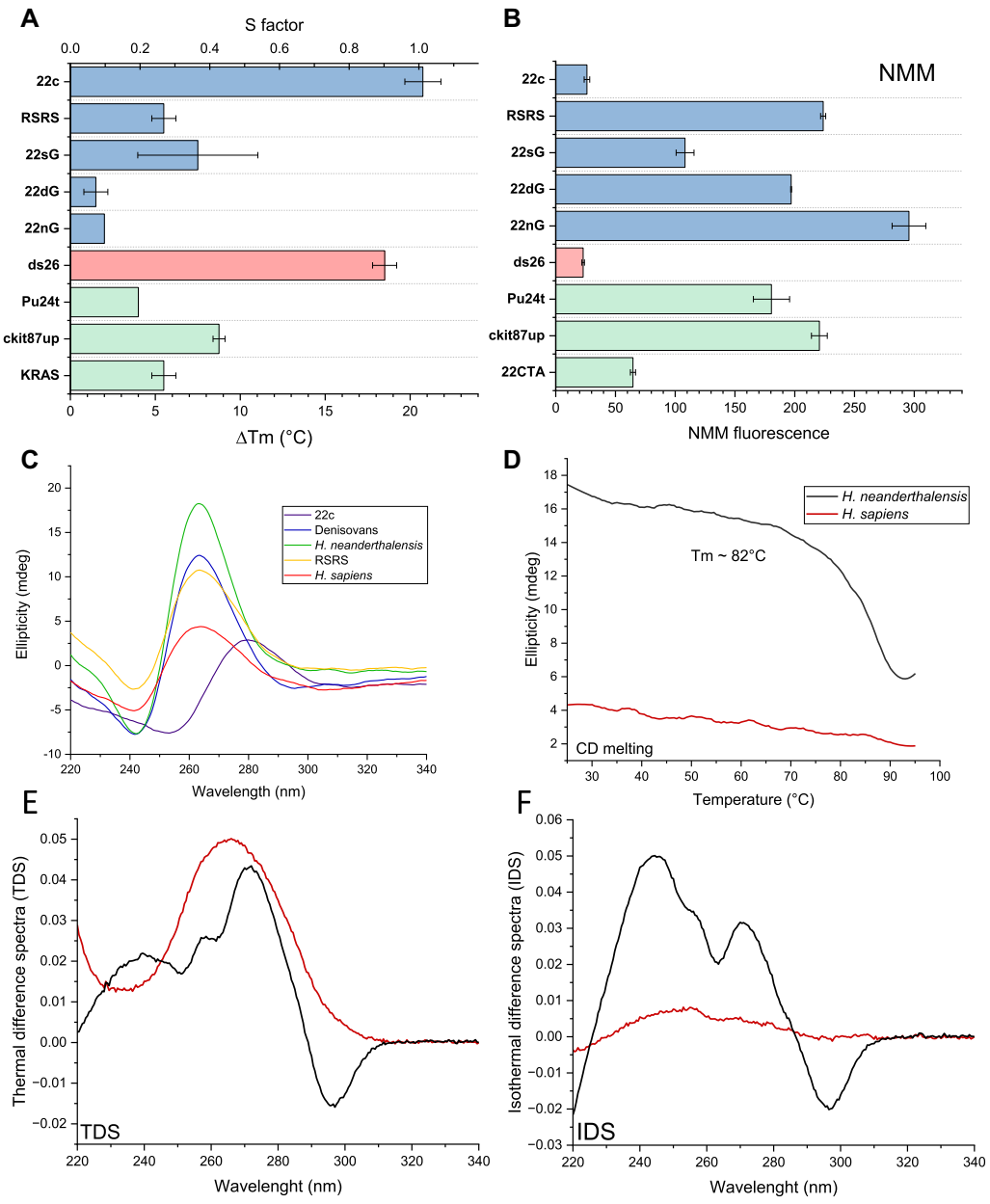


**Figure 2.** Experimental confirmation of G4 formation. (**A**) FRET-MC assay: in a microplate were mixed 0.2 μM of double labeled F21T, 3 μM of the pre-folded sequences in 10mM lithium cacodylate supplemented with 10mM KCl with or without 0.4 μM PhenDC3. Known G4-forming (in green, Pu24t, ckit87up, KRAS) or non-G4 forming (in red, ds26) controls were tested in parallel. Positive G4-forming sequences act as potent inhibitors, leading to a decrease in *S*-factor. Mean values of delta Tm ± SD are indicated for each group. 'n' stands for *H. neanderthalensis*, 's' for *H. sapiens*. Control sequences are shown in Supplementary Table S2. (**B**) Column bar graph representing NMM fluorescence intensity: in a microplate were mixed 2 μM of NMM with 3 μM of the pre-folded sequence in 10 mM lithium cacodylate supplemented with 100 mM KCl. NMM fluorescence increases in the presence of a quadruplex structure. Error bars correspond to the SD calculated from two replicates. (**C**) Circular dichroism spectra recorded at 25°C (3 μM strand concentration) in a 10 mM lithium cacodylate buffer supplemented with 100 mM KCl. (**D**) CD melting recorded in 25–95°C temperature range at 260 nm. A clear transition is observed for *H. neanderthalensis*, not the *H. sapiens* motif. (**E**) Thermal difference spectra (TDS) and (**F**) isothermal difference spectra (IDS) are the arithmetic difference of two spectra recorded in unfavorable G4 formation and in G4 promoting conditions. In panels (D–F) the *H. neanderthalensis* motif is shown in light blue, *H. sapiens* in red. Both TDS and IDS curves for *H. neanderthalensis* are indicative of G4 formation, in contrast to the *H. sapiens* profile.

- The NMM fluorescence light-up assay (Figure 2B) shows a significant differential behavior between the different sequences tested. Additional controls were included, including G4-forming samples (22Ag to cmyc) and non G4-forming negative controls, such as RND6, ds26 or 22c, the later corresponding to the mtDNA negative control in which G4 formation is not possible. The fluorescence signal increased in the order 22c < 22sG < 22dG < 22nG, suggesting increasing G4 formation in this order, with the highest level observed for 22nG.
- Circular dichroism (CD) spectra of the 22 long oligonucleotides revealed interesting differences (Figure 2C). The negative control sequence 22c exhibited a spectra typical of a unstructured sequence. In contrast, the CD spectra of the *H. neanderthalensis* sequence closely matches what would be expected for a parallel G-quadruplex (58) (e.g. a positive peak around 260 nm), while the other sequences (22sG, 22sG and RSRS) exhibited an intermediate behavior, with a positive peak of lower intensity at 260 nm, suggesting partial or incomplete G4 formation for these sequences. Interestingly, when increasing temperature, a clear inverted transition was observed around 85°C for the *H. neanderthalensis* sequence, demonstrating high thermal stability of this sequence. In contrast, the Denisovans and *H. sapiens* sequences exhibited a lower $T_m$ or no clear transition, respectively (Figure 2D and Supplementary Figure S3).
- Isothermal (IDS; Figure 2F) and Thermal (TDS, Figure 2E) difference spectra of the 22nG sequences closely matched the IDS and TDS of a G-quadruplex (58,64), confirming G4 formation for this sequence. The IDS and TDS of all other sequences were either inconclusive or incompatible with G4 formation (Supplementary Figures S4 and S5).
- Finally, non denaturing gel electrophoresis (Supplementary Figure S6) confirmed a different behavior of the *H. neanderthalensis* sequence when compared to the *H. sapiens* or Denisovans ones.

Altogether, the results shown in Figure 2 and Supplementary Figure S3-S6 indicate that the *H. neanderthalensis* sequence is more prone to G4 formation than its Denisovans or *H. sapiens* counterparts.

Qualitatively similar results were obtained when comparing *H. sapiens* and *H. neanderthalensis* longer sequences (31 oligonucleotides) (Supplementary Figure S7). We found a differential tendency of the *H. sapiens* and *H. neanderthalensis* sequences to form G-quadruplexes; 31nG being more prone to form highly stable parallel G4 than its *H. sapiens* counterpart. A clear difference of behavior was again found by gel electrophoresis between the *H. neanderthalensis* and *H. sapiens* sequences. This technique told a slightly more complicated story, as multiple bands, corresponding to multiple quadruplexes of different molecularities were found for 31nG, while a less variations was found for 31sG.

The formation of multiple and/or higher-order G-quadruplex structures by oligonucleotides containing a long uninterrupted run of guanines is in agreement with the observations of Phan and colleagues (61), who observed that long poly-G sequences often lead to multiple possible ways of G-quadruplex folding, rendering their structural characterization challenging. One exception was d($TTG_{15}T$), which formed a well-defined intramolecular parallel G4 structure with three G-quartets and three single-guanine propeller loops (61). The d($G_{12}$) motif present in the *H. neanderthalensis* sequences gives rise to multiple arrangements. Overall, the comparison of synthetic oligonucleotides of different lengths (22 and 21 nucleotide-long) confirmed a clear difference in behavior between the *H. neanderthalensis* sequence on the one hand, and the *H. sapiens* and *Denisovans* motifs on the other hand. Thanks to its uninterrupted poly-G run, the *H. neanderthalensis* motif is more prone to form stable G-quadruplexes than the others.

## Discussion

Mitochondria are responsible for producing energy in the form of ATP through cellular respiration. Mitochondrial dysfunction is involved in a number of diseases and this dysfunction may be the result of variations of the mitochondrial DNA sequence. Mutations in mtDNA can lead to failure in the electron transport chain, which can result in reduced ATP production and the accumulation of reactive oxygen species. These defects in mitochondrial metabolism can cause a variety of diseases, including mitochondrial myopathies, encephalopathies, and neuropathies. Mutations in mtDNA have also been associated with age-related pathologies in *H. sapiens*, such as Parkinson's disease, Alzheimer's disease, and diabetes. In some cases, single-base mutations in mtDNA can alter G4 formation *in vitro* (65).

Of critical importance seems to be the D-loop corresponding to the OriB origin of replication. Mutations in this region (at position 16,189 in particular), have been associated with both early growth and adult metabolic phenotypes. Sequence variants are relatively frequent in this region: for example, the T > C nucleotide transition at mt16189 represents 24.5% of all sequences uploaded in Mitomap (https://www.mitomap.org/MITOMAP). This SNP has a critical impact on potential G4 formation. The *H. sapiens* reference genome has a standard sequence composed of two short C tracks (5 and 4 Cs separated by one T). The T > C nucleotide transition leads to an interrupted track of 10 cytosines, and this T > C transition can generate a variable length polycytosine tract (poly-C).

This means that its complementary strand would contain 10 guanines or more in a row and become more prone to G4 formation. It has been demonstrated that the number of potential G4-forming sequences in the mitochondrial genome increases with the evolutionary complexity of different species (66) and that the conservation of G4s points to their regulation and function of mtDNA (43). The Brosh team demonstrated that DNA synthesis by two mitochondrial DNA polymerases can be blocked by stable G4 mitochondrial DNA structures (67) that could be overcome by the G4-resolving helicase Pif1. However, error-prone DNA synthesis by PrimPol using a G4 template sequence persisted even in the presence of Pif1. The same team found that the mitochondrial G-rich sequences found near deletion breakpoints form G-quadruplex DNA structures. They suggest that mitochondrial G4 are likely to be a source of genomic instability by perturbing the normal progression of the mitochondrial replication machinery (68). Sullivan *et al.* also identified a G4 sequence at the heavy-strand promoter (HSP1) that has the potential to cause significant stalling of mtDNA replication (69). G4 ligands can perturb mitochondrial genome replication, transcription processivity, and respiratory function in normal cells (70). G4 formation between nascent RNA and the non-

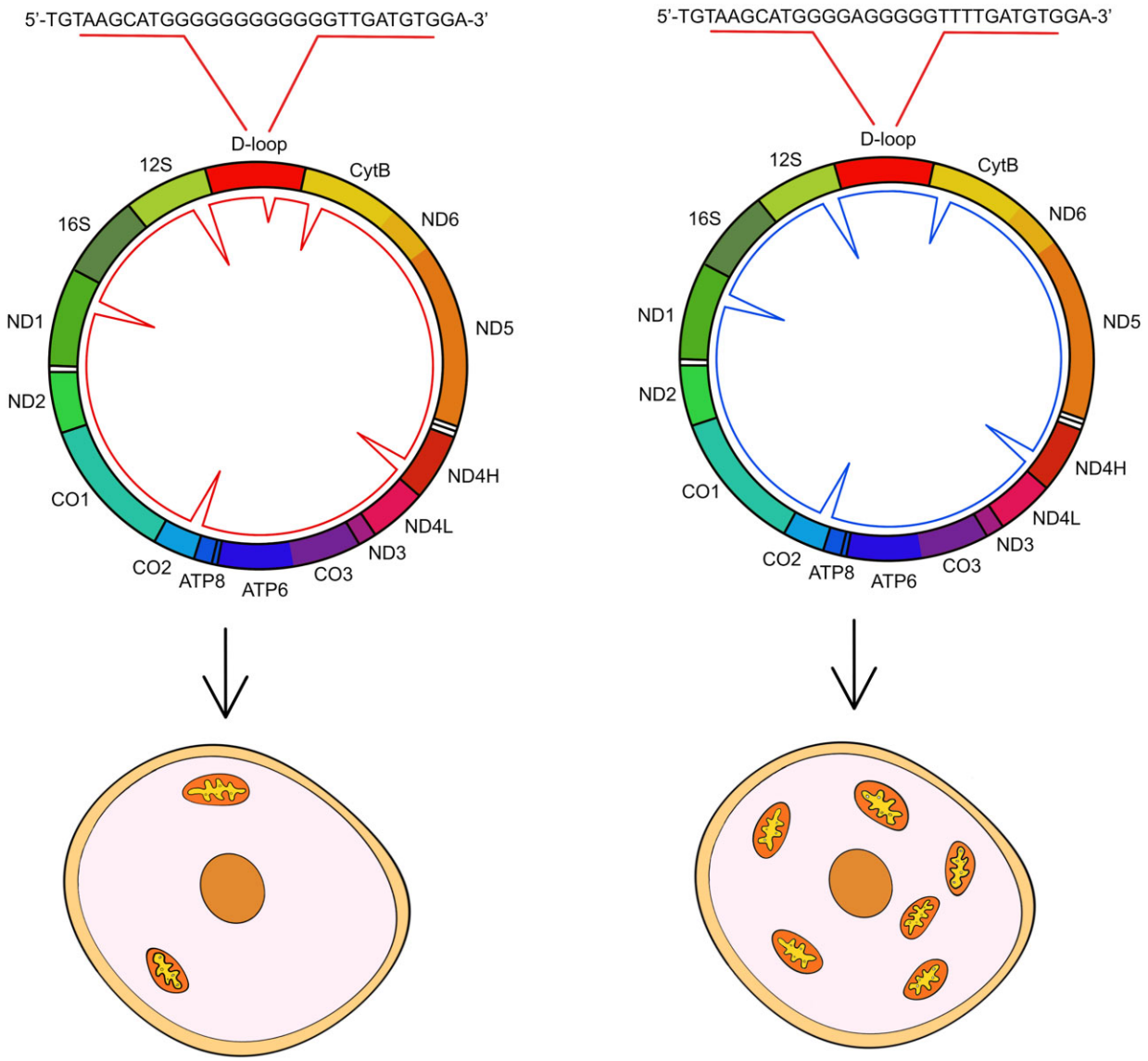


**Figure 3.** A decreased mtDNA copy number may be associated with an increased number of continuous cytosine within the 16180–16195 segment (79).

template DNA strand in this region may decide the rate of initiation of DNA synthesis in human mitochondria (71) while RNA G4 structures can stimulate mitochondrial transcription termination and primer formation (72). Evidence for G4 formation in live mitochondria has been provided by fluorescent light-up probes such as BMVC (73). All these results point out to the importance of G4 structures in the mitochondrial genome (74).

The physiological impact of the T > C nucleotide transition at mt16189 has been studied in *H. sapiens* for various pathologies such as cancer, endometriosis or metabolic diseases including diabetes and obesity. Several studies concluded that mitochondrial D-loop alterations may constitute inherent risk factors for these diseases, although ethnic differences were observed. This tract variance has been associated with different pathologies (68,69 76). Mitochondrial C-tract changes were identified as a clonal relationship in patients with squamous carcinoma (77). Mutations in the D-loop that increase the length of the C-track also correlate with an increase in diabetes mellitus (78) and lacunar cerebral infarction (75). Interestingly, the mtDNA 16189 variant and more generally the presence of an uninterrupted poly-C run in this region can cause strong decrease of mtDNA copy number in human blood cells (79), indicating that an uninterrupted poly-C/poly-G long run in the D-loop region poses problems to mtDNA replication (Figure 3). Furthermore, G-quadruplex formation in mtDNA has been shown to inhibit replication fork progression and leads to loss of mtDNA in human cells (42).

It is interesting to compare the mtDNA genome of *H. sapiens*, Denisovans and *H. neanderthalensis* in the light of these observations. While the overall PQS density is almost identical between these mitochondrial reference genomes, a notable difference is found in the D-loop region. *H. neanderthalensis* contains a very G4-prone motif in this region, with a G4Hunter score >2, significantly above the G4Hunter scores for the *H. sapiens* and Denisovans motifs found in this region. A high score means that stable G4 are formed in 100% of the cases (55). In this manuscript, we could confirm by a number of independent methods that the *H. neanderthalensis* sequence was highly prone to G4 formation, with species of various molec-

ularities and high thermal stabilities. It was important to use a combination of techniques to avoid technical pitfalls (58), or inherent limitations such as the need to use non physiological potassium concentrations (note, however, that the intramitochondrial potassium concentration may differ from the cytoplasm). Overall, these approaches gave consistent results indicating that the *H. neanderthalensis* motif was more likely to form high stability quadruplexes that may cause problems during replication. It was indeed shown that D-loop G-rich variant leads to decreased mitochondrial copy number in *H. sapiens* peripheral blood cells. The evidence is indeed correlative; yet, subjects harbouring a variant uninterrupted poly-G showed lowest mtDNA copy number while an increased copy number was noted in subjects harbouring standard interrupted poly-G variant. Yet, this observation was reported in an *H. sapiens* context; its relevance for *H. neanderthalensis* remains to be demonstrated but is currently not technically feasible: for example, we would have to work on cells expressing the *H. neanderthalensis* versions of all mitochondrial G4-binding proteins and G4-helicases to determine how detrimental would be this uninterrupted G-track in *H. neanderthalensis*.

In the same vein, coordinated replication and expression of mitochondrial genome is critical for metabolically active cells. Terniakov and colleagues have found that interaction of *H. sapiens* transcription elongation factor, TEFM with mitochondrial RNA polymerase and nascent transcript prevents generation of replication primers and increases transcription processivity (80). It would be interesting to study if a similar molecular switch between replication and transcription occurs in *H. neanderthalensis* mitochondria. Again, to be valid, this study should be performed in a *H. neanderthalensis* genomic and proteomic context.

The uninterrupted allele may be found in *H. sapiens*, although with a very low frequency. This allele has been associated with a lower replication rate of mtDNA, a lower number of mitochondrias, and various pathologies. Unless *H. neanderthalensis* was better equipped to deal with polyG/polyC tracks in its mitochondrial genome than *H. sapiens*, this allele may have had a detrimental effect on *H. neanderthalensis* fitness and perhaps constitute an evolutionary disadvantage.

## Conclusions

Modern sequencing methods allowed us to obtain information about the genome of extinct *H. neanderthalensis* and Denisovans in relation to *H. sapiens*. Analysis of G-quadruplexes in these genomes showed that the number of PQS in mtDNA was similar in all cases, with one important difference for the very stable G4-forming sequence in the D-loop of the *H. neanderthalensis* mitochondrial genome. As this D-loop region plays crucial function for mtDNA replication, the presence of a predominant long G-track in *H. neanderthalensis* mtDNA possibly constituted a deleterious evolutionary disadvantage.

## Data availability

All sequences studied are publicly available in the NCBI database. Genbank accession numbers, oligonucleotide sequences and data analyses are available in the article or Supplementary tables and figures. Raw spectra, non-denaturing gels and melting curves are presented in supplementary information.

## Supplementary data

Supplementary Data are available at NARGAB Online.

## Acknowledgements

We thank Lionel Guittat, Rongxin Zhang (LOB, Palaiseau, France), Dominique Grimaud-Hervé (*Musée de l'Homme*, Paris, France) for helpful discussions. This work has been conducted in the sustainability period of the project SYMBIT No. CZ.02.1.01/0.0/0.0/15_003/0000477 as its follow-up activity .

## Funding

Czech Science Foundation [22-21903S]; INCa PL-BIO [2020-117]; ANR grants [ANR-20-CE12-0023]; G4Access. Funding for open access charge: INCa.

## Conflict of interest statement

None declared.

## References

1. Harvati,K., Gunz,P. and Grigorescu,D. (2007) Cioclovina (Romania): affinities of an early modern European. *J. Hum. Evol.*, **53**, 732–746.
2. Soficaru,A., Doboş,A. and Trinkaus,E. (2006) Early modern humans from the Peştera Muierii, Baia de Fier, Romania. *Proc. Natl. Acad. Sci. USA*, **103**, 17196–17201.
3. Prüfer,K., de Filippo,C., Grote,S., Mafessoni,F., Korlević,P., Hajdinjak,M., Vernot,B., Skov,L., Hsieh,P., Peyrégne,S., *et al.* (2017) A high-coverage Neandertal genome from Vindija Cave in Croatia. *Science*, **358**, 655–658.
4. Prüfer,K., Racimo,F., Patterson,N., Jay,F., Sankararaman,S., Sawyer,S., Heinze,A., Renaud,G., Sudmant,P.H., de Filippo,C., *et al.* (2014) The complete genome sequence of a Neanderthal from the Altai Mountains. *Nature*, **505**, 43–49.
5. Green,R.E., Malaspinas,A.-S., Krause,J., Briggs,A.W., Johnson,P.L.F., Uhler,C., Meyer,M., Good,J.M., Maricic,T., Stenzel,U., *et al.* (2008) A complete Neandertal mitochondrial genome sequence determined by high-throughput sequencing. *Cell*, **134**, 416–426.
6. Serre,D., Langaney,A., Chech,M., Teschler-Nicola,M., Paunovic,M., Mennecier,P., Hofreiter,M., Possnert,G. and Pääbo,S. (2004) No evidence of Neandertal mtDNA contribution to early modern humans. *PLoS Biol.*, **2**, e57.
7. Briggs,A.W., Good,J.M., Green,R.E., Krause,J., Maricic,T., Stenzel,U., Lalueza-Fox,C., Rudan,P., Brajković,D., Kućan,Ž., *et al.* (2009) Targeted retrieval and analysis of five Neandertal mtDNA genomes. *Science*, **325**, 318–321.
8. Mafessoni,F., Grote,S., De Filippo,C., Slon,V., Kolobova,K.A., Viola,B., Markin,S.V., Chintalapati,M., Peyrégne,S., Skov,L., *et al.* (2020) A high-coverage Neandertal genome from Chagyrskaya Cave. *Proc. Natl. Acad. Sci. USA*, **117**, 15132–15136.
9. Hajdinjak,M., Fu,Q., Hübner,A., Petr,M., Mafessoni,F., Grote,S., Skoglund,P., Narasimham,V., Rougier,H., Crevecoeur,I., *et al.* (2018) Reconstructing the genetic history of late Neanderthals. *Nature*, **555**, 652–656.
10. Wall,J.D., Yang,M.A., Jay,F., Kim,S.K., Durand,E.Y., Stevison,L.S., Gignoux,C., Woerner,A., Hammer,M.F. and Slatkin,M. (2013)

Higher levels of Neanderthal ancestry in East Asians than in Europeans. *Genetics*, **194**, 199–209.
11. Sankararaman,S., Mallick,S., Dannemann,M., Prüfer,K., Kelso,J., Pääbo,S., Patterson,N. and Reich,D. (2014) The genomic landscape of Neanderthal ancestry in present-day humans. *Nature*, **507**, 354–357.
12. Reich,D., Green,R.E., Kircher,M., Krause,J., Patterson,N., Durand,E.Y., Viola,B., Briggs,A.W., Stenzel,U., Johnson,P.L.F., *et al.* (2010) Genetic history of an archaic hominin group from Denisova Cave in Siberia. *Nature*, **468**, 1053–1060.
13. Fu,Q., Li,H., Moorjani,P., Jay,F., Slepchenko,S.M., Bondarev,A.A., Johnson,P.L.F., Aximu-Petri,A., Prüfer,K., De Filippo,C., *et al.* (2014) Genome sequence of a 45,000-year-old modern human from western Siberia. *Nature*, **514**, 445–449.
14. Reilly,P.F., Tjahjadi,A., Miller,S.L., Akey,J.M. and Tucci,S. (2022) The contribution of Neanderthal introgression to modern human traits. *Curr. Biol.*, **32**, R970–R983.
15. Deschamps,M., Laval,G., Fagny,M., Itan,Y., Abel,L., Casanova,J.-L., Patin,E. and Quintana-Murci,L. (2016) Genomic signatures of selective pressures and introgression from archaic hominins at human innate immunity genes. *Am. Hum. Genet.*, **98**, 5–21.
16. Enard,D. and Petrov,D.A. (2018) Evidence that RNA viruses drove adaptive introgression between Neanderthals and modern humans. *Cell*, **175**, 360–371.
17. Zhang,X., Witt,K.E., Bañuelos,M.M., Ko,A., Yuan,K., Xu,S., Nielsen,R. and Huerta-Sanchez,E. (2021) The history and evolution of the Denisovan- *EPAS1* haplotype in Tibetans. *Proc. Natl. Acad. Sci. U.S.A.*, **118**, e2020803118.
18. International Human Genome Sequencing Consortium, Whitehead Institute for Biomedical Research, Center for Genome Research, Lander,E.S., Linton,L.M., Birren,B., Nusbaum,C., Zody,M.C., Baldwin,J., Devon,K., Dewar,K., *et al.* (2001) Initial sequencing and analysis of the human genome. *Nature*, **409**, 860–921.
19. Venter,J.C., Adams,M.D., Myers,E.W., Li,P.W., Mural,R.J., Sutton,G.G., Smith,H.O., Yandell,M., Evans,C.A., Holt,R.A., *et al.* (2001) The sequence of the human genome. *Science*, **291**, 1304–1351.
20. Nurk,S., Koren,S., Rhie,A., Rautiainen,M., Bzikadze,A.V., Mikheenko,A., Vollger,M.R., Altemose,N., Uralsky,L., Gershman,A., *et al.* (2022) The complete sequence of a human genome. *Science*, **376**, 44–53.
21. Kerner,G., Patin,E. and Quintana-Murci,L. (2021) New insights into human immunity from ancient genomics. *Curr. Opin. Immunol.*, **72**, 116–125.
22. Mergny,J.-L. and Sen,D. (2019) DNA quadruple helices in nanotechnology. *Chem. Rev.*, **119**, 6290–6325.
23. Wong,A. and Wu,G. (2003) Selective binding of monovalent cations to the stacking G-quartet structure formed by guanosine 5‘-monophosphate: a solid-state NMR study. *J. Am. Chem. Soc.*, **125**, 13895–13905.
24. Harkness,R.W. and Mittermaier,A.K. (2017) G-quadruplex dynamics. *Biochim. Biophys. Acta (BBA) - Proteins Proteomics*, **1865**, 1544–1554.
25. Bartas,M., Čutová,M., Brázda,V., Kaura,P., Šťastný,J., Kolomazník,J., Coufal,J., Goswami,P., Červeň,J. and Pečinka,P. (2019) The presence and localization of G-quadruplex forming sequences in the domain of bacteria. *Molecules*, **24**, 1711.
26. Bohálová,N., Mergny,J.-L. and Brázda,V. (2021) Novel G-quadruplex prone sequences emerge in the complete assembly of the human X chromosome. *Biochimie*, **191**, 87–90.
27. Brázda,V., Luo,Y., Bartas,M., Kaura,P., Porubiaková,O., Šťastný,J., Pečinka,P., Verga,D., Da Cunha,V., Takahashi,T.S., *et al.* (2020) G-quadruplexes in the archaea domain. *Biomolecules*, **10**, 1349.
28. Chashchina,G.V., Shchyolkina,A.K., Kolosov,S.V., Beniaminov,A.D. and Kaluzhny,D.N. (2021) Recurrent potential G-quadruplex sequences in archaeal genomes. *Front. Microbiol.*, **12**, 647851.
29. Cueny,R.R., McMillan,S.D. and Keck,J.L. (2022) G-quadruplexes in bacteria: insights into the regulatory roles and interacting proteins of non-canonical nucleic acid structures. *Crit. Rev. Biochem. Mol. Biol.*, **57**, 539–561.
30. Dobrovolná,M., Bohálová,N., Peška,V., Wang,J., Luo,Y., Bartas,M., Volná,A., Mergny,J.-L. and Brázda,V. (2022) The newly sequenced genome of *Pisum sativum* is replete with potential G-quadruplex-forming sequences—implications for evolution and biological regulation. *Int. J. Mol. Sci.*, **23**, 8482.
31. Griffin,B.D. and Bass,H.W. (2018) Plant G-quadruplex (G4) motifs in DNA and RNA; abundant, intriguing sequences of unknown function. *Plant Sci.*, **269**, 143–147.
32. Huppert,J.L. (2005) Prevalence of quadruplexes in the human genome. *Nucleic Acids Res.*, **33**, 2908–2916.
33. Zhang,Z.-H., Qian,S.H., Wei,D. and Chen,Z.-X. (2023) In vivo dynamics and regulation of DNA G-quadruplex structures in mammals. *Cell Biosci.*, **13**, 117.
34. Rhodes,D. and Lipps,H.J. (2015) G-quadruplexes and their regulatory roles in biology. *Nucleic Acids Res.*, **43**, 8627–8637.
35. Galli,S., Melidis,L., Flynn,S.M., Varshney,D., Simeone,A., Spiegel,J., Madden,S.K., Tannahill,D. and Balasubramanian,S. (2022) DNA G-quadruplex recognition in vitro and in live cells by a structure-specific manobody. *J. Am. Chem. Soc.*, **144**, 23096–23103.
36. Jansson,L.I., Hentschel,J., Parks,J.W., Chang,T.R., Lu,C., Baral,R., Bagshaw,C.R. and Stone,M.D. (2019) Telomere DNA G-quadruplex folding within actively extending human telomerase. *Proc. Natl. Acad. Sci. U.S.A.*, **116**, 9350–9359.
37. Raguseo,F., Chowdhury,S., Minard,A. and Di Antonio,M. (2020) Chemical-biology approaches to probe DNA and RNA G-quadruplex structures in the genome. *Chem. Commun.*, **56**, 1317–1324.
38. Brázda,V., Bohálová,N. and Bowater,R.P. (2022) New telomere to telomere assembly of human chromosome 8 reveals a previous underestimation of G-quadruplex forming sequences and inverted repeats. *Gene*, **810**, 146058.
39. Kang,Y. and Wei,C. (2022) A stilbene derivative as dual-channel fluorescent probe for mitochondrial G-quadruplex DNA in living cells. *Spectrochim. Acta Part A*, **278**, 121316.
40. Varshney,D., Spiegel,J., Zyner,K., Tannahill,D. and Balasubramanian,S. (2020) The regulation and functions of DNA and RNA G-quadruplexes. *Nat. Rev. Mol. Cell Biol.*, **21**, 459–474.
41. Bedrat,A., Lacroix,L. and Mergny,J.-L. (2016) Re-evaluation of G-quadruplex propensity with G4Hunter. *Nucleic Acids Res.*, **44**, 1746–1759.
42. Doimo,M., Chaudhari,N., Abrahamsson,S., L'Hôte,V., Nguyen,T.V.H., Berner,A., Ndi,M., Abrahamsson,A., Das,R.N., Aasumets,K., *et al.* (2023) Enhanced mitochondrial G-quadruplex formation impedes replication fork progression leading to mtDNA loss in human cells. *Nucleic Acids Res.*, **51**, 7392–7408.
43. Bohálová,N., Dobrovolná,M., Brázda,V. and Bidula,S. (2022) Conservation and over-representation of G-quadruplex sequences in regulatory regions of mitochondrial DNA across distinct taxonomic sub-groups. *Biochimie*, **194**, 28–34.
44. Cavalcante,G.C., Magalhães,L., Ribeiro-dos-Santos,Â. and Vidal,A.F. (2020) Mitochondrial epigenetics: non-coding RNAs as a novel layer of complexity. *Int. J. Mol. Sci.*, **21**, 1838.
45. Liu,C.-C., Fang,T.-J., Ou,T.-T., Wu,C.-C., Li,R.-N., Lin,Y.-C., Lin,C.-H., Tsai,W.-C., Liu,H.-W. and Yen,J.-H. (2011) Global DNA methylation, DNMT1, and MBD2 in patients with rheumatoid arthritis. *Immunol. Lett.*, **135**, 96–99.
46. Guo,X., Jing,C., Li,L., Zhang,L., Shi,Y., Wang,J., Liu,J. and Li,C. (2011) Down-regulation of VEZT gene expression in human gastric cancer involves promoter methylation and miR-43c. *Biochem. Biophys. Res. Commun.*, **404**, 622–627.
47. Zhang,J., Zhang,J., Lai,R., Peng,C., Guo,Z. and Wang,C. (2023) Risk-associated single nucleotide polymorphisms of mitochondrial D-loop mediate imbalance of cytokines and redox in rheumatoid arthritis. *Int. J of Rheum. Dis.*, **26**, 124–131.

48. Zhao,Y., Peng,C., Lai,R., Zhang,J., Zhang,X. and Guo,Z. (2022) The SNPs of mitochondrial DNA displacement loop region and mitochondrial DNA copy number associated with risk of polymyositis and dermatomyositis. *Sci. Rep.*, **12**, 5903.
49. Zhao,Y., Peng,C., Zhang,J., Lai,R., Zhang,X. and Guo,Z. (2022) Mitochondrial displacement loop region SNPs modify Sjögren's syndrome development by regulating cytokines expression in female patients. *Front. Genet.*, **13**, 847521.
50. Mposhi,A., Liang,L., Mennega,K.P., Yildiz,D., Kampert,C., Hof,I.H., Jellema,P.G., De Koning,T.J., Faber,K.N., Ruiters,M.H.J., *et al.* (2022) The mitochondrial epigenome: an unexplored avenue to explain unexplained myopathies? *Int. J. Mol. Sci.*, **23**, 2197.
51. Lai,R., Zhang,X., Qiao,K., Gao,X., Li,S., Zhang,R., Qi,Y. and Peng,C. (2021) Identification of sequence polymorphisms in the mitochondrial deoxyribonucleic acid displacement-loop region as risk factors for systemic lupus erythematosus. *Arch. Rheumatol.*, **36**, 375–380.
52. Stoccoro,A., Smith,A.R., Baldacci,F., Del Gamba,C., Lo Gerfo,A., Ceravolo,R., Lunnon,K., Migliore,L. and Coppedè,F. (2021) Mitochondrial D-loop region methylation and copy number in peripheral blood DNA of Parkinson's disease patients. *Genes*, **12**, 720.
53. Yang,H. (2012) Correlation between increased ND2 expression and demethylated displacement loop of mtDNA in colorectal cancer. *Mol. Med. Rep.*, **6**, 125–130.
54. Nicholls,T.J. and Minczuk,M. (2014) In D-loop: 40years of mitochondrial 7S DNA. *Exp. Gerontol.*, **56**, 175–181.
55. Esnault,C., Magat,T., Zine El Aabidine,A., Garcia-Oliver,E., Cucchiarini,A., Bouchouika,S., Lleres,D., Goerke,L., Luo,Y., Verga,D., *et al.* (2023) G4access identifies G-quadruplexes and their associations with open chromatin and imprinting control regions. *Nat. Genet.*, **55**, 1359–1369.
56. Okonechnikov,K., Golosova,O., Fursov,M. and the UGENE teamthe UGENE team (2012) Unipro UGENE: a unified bioinformatics toolkit. *Bioinformatics*, **28**, 1166–1167.
57. Crooks,G.E., Hon,G., Chandonia,J.-M. and Brenner,S.E. (2004) WebLogo: a sequence logo generator: Figure 1. *Genome Res.*, **14**, 1188–1190.
58. Luo,Y., Granzhan,A., Marquevielle,J., Cucchiarini,A., Lacroix,L., Amrane,S., Verga,D. and Mergny,J.-L. (2022) Guidelines for G-quadruplexes: I. In vitro characterization. *Biochimie*, **214**, 5–23
59. Renaud De La Faverie,A., Guédin,A., Bedrat,A., Yatsunyk,L.A. and Mergny,J.-L. (2014) Thioflavin T as a fluorescence light-up probe for G4 formation. *Nucleic Acids Res.*, **42**, e65.
60. Zhang,Z., Schwartz,S., Wagner,L. and Miller,W. (2000) A greedy algorithm for aligning DNA sequences. *J. Comput. Biol.*, **7**, 203–214.
61. Sengar,A., Heddi,B. and Phan,A.T. (2014) Formation of G-quadruplexes in poly-G sequences: structure of a propeller-type parallel-stranded G-quadruplex formed by a $G_{15}$ stretch. *Biochemistry*, **53**, 7718–7723.
62. Behar,D.M., van Oven,M., Rosset,S., Metspalu,M., Loogväli,E.-L., Silva,N.M., Kivisild,T., Torroni,A. and Villems,R. (2012) A "Copernican" reassessment of the human mitochondrial DNA tree from its root. *Am. Hum. Genet.*, **90**, 675–684.
63. Luo,Y., Granzhan,A., Verga,D. and Mergny,J. (2021) FRET-MC: a fluorescence melting competition assay for studying G4 structures in vitro. *Biopolymers*, **112**, e23415.
64. Mergny,J.-L. (2005) Thermal difference spectra: a specific signature for nucleic acid structures. *Nucleic Acids Res.*, **33**, e138.
65. Chu,I.-T., Wu,C.-C. and Chang,T.-C. (2019) G-quadruplex formation by single-base mutation or deletion of mitochondrial DNA sequences. *Biochim. Biophys. Acta*, **1863**, 418–425.
66. Sahayasheela,V.J., Yu,Z., Hidaka,T., Pandian,G.N. and Sugiyama,H. (2023) Mitochondria and G-quadruplex evolution: an intertwined relationship. *Trends Genet.*, **39**, 15–30.
67. Butler,T.J., Estep,K.N., Sommers,J.A., Maul,R.W., Moore,A.Z., Bandinelli,S., Cucca,F., Tuke,M.A., Wood,A.R., Bharti,S.K., *et al.* (2020) Mitochondrial genetic variation is enriched in G-quadruplex regions that stall DNA synthesis in vitro. *Hum. Mol. Genet.*, **29**, 1292–1309.
68. Bharti,S.K., Sommers,J.A., Zhou,J., Kaplan,D.L., Spelbrink,J.N., Mergny,J.-L. and Brosh,R.M. (2014) DNA sequences proximal to human mitochondrial DNA deletion breakpoints prevalent in human disease form G-quadruplexes, a class of DNA structures inefficiently unwound by the mitochondrial replicative twinkle helicase. *J. Biol. Chem.*, **289**, 29975–29993.
69. Sullivan,E.D., Longley,M.J. and Copeland,W.C. (2020) Polymerase $\gamma$ efficiently replicates through many natural template barriers but stalls at the HSP1 quadruplex. *J. Biol. Chem.*, **295**, 17802–17815.
70. Falabella,M., Kolesar,J.E., Wallace,C., De Jesus,D., Sun,L., Taguchi,Y.V., Wang,C., Wang,T., Xiang,I.M., Alder,J.K., *et al.* (2019) G-quadruplex dynamics contribute to regulation of mitochondrial gene expression. *Sci. Rep.*, **9**, 5605.
71. Wanrooij,P.H., Uhler,J.P., Shi,Y., Westerlund,F., Falkenberg,M. and Gustafsson,C.M. (2012) A hybrid G-quadruplex structure formed between RNA and DNA explains the extraordinary stability of the mitochondrial R-loop. *Nucleic Acids Res.*, **40**, 10334–10344.
72. Wanrooij,P.H., Uhler,J.P., Simonsson,T., Falkenberg,M. and Gustafsson,C.M. (2010) G-quadruplex structures in RNA stimulate mitochondrial transcription termination and primer formation. *Proc. Natl. Acad. Sci. U.S.A.*, **107**, 16072–16077.
73. Huang,W.-C., Tseng,T.-Y., Chen,Y.-T., Chang,C.-C., Wang,Z.-F., Wang,C.-L., Hsu,T.-N., Li,P.-T., Chen,C.-T., Lin,J.-J., *et al.* (2015) Direct evidence of mitochondrial G-quadruplex DNA by using fluorescent anti-cancer agents. *Nucleic Acids Res.*, **43**, 10102–10113.
74. Falabella,M., Fernandez,R.J., Johnson,F.B. and Kaufman,B.A. (2019) Potential roles for G-quadruplexes in mitochondria. *CMC*, **26**, 2918–2932.
75. Liou,C.-W., Lin,T.-K., Huang,F.-M., Chen,T.-L., Lee,C.-F., Chuang,Y.-C., Tan,T.-Y., Chang,K.-C. and Wei,Y.-H. (2004) Association of the mitochondrial DNA 16189 T to C variant with lacunar cerebral infarction: evidence from a hospital-based case-control study. *Ann. N. Y. Acad. Sci.*, **1011**, 317–324.
76. Pandey,R., Mehrotra,D., Mahdi,A.A., Sarin,R. and Kowtal,P. (2014) Additional cytosine inside mitochondrial C-tract D-loop as a progression risk factor in oral precancer cases. *J. Oral Biol. Craniof. Res.*, **4**, 3–7.
77. Ha,P.K., Tong,B.C., Westra,W.H., Sanchez-Cespedes,M., Parrella,P., Zahurak,M., Sidransky,D. and Califano,J.A. (2002) Mitochondrial C-tract alteration in premalignant lesions of the head and neck: a marker for progression and clonal proliferation. *Clin. Cancer Res.*, **8**, 2260–2265.
78. Tang,D., Zhou,X., Zhou,K., Li,X., Zhao,L., Liu,F., Zheng,F. and Liu,S. (2005) [Association of mitochondrial DNA variation with type 2 diabetes mellitus]. *Zhonghua Yi Xue Yi Chuan Xue Za Zhi*, **22**, 636–640.
79. Liou,C.-W., Lin,T.-K., Chen,J.-B., Tiao,M.-M., Weng,S.-W., Chen,S.-D., Chuang,Y.-C., Chuang,J.-H. and Wang,P.-W. (2010) Association between a common mitochondrial DNA D-loop polycytosine variant and alteration of mitochondrial copy number in human peripheral blood cells. *J. Med. Genet.*, **47**, 723–728.
80. Agaronyan,K., Morozov,Y.I., Anikin,M. and Temiakov,D. (2015) Mitochondrial biology. Replication-transcription switch in human mitochondria. *Science*, **347**, 548–551.


**Received:** December 15, 2023. **Revised:** April 18, 2024. **Editorial Decision:** May 13, 2024. **Accepted:** May 17, 2024